

Giant magnetoelectric effect in sintered multilayered composite structures

Rashed A. Islam, Yong Ni, Armen G. Khachatryan, and Shashank Priya

Citation: *Journal of Applied Physics* **104**, 044103 (2008); doi: 10.1063/1.2966597

View online: <http://dx.doi.org/10.1063/1.2966597>

View Table of Contents: <http://scitation.aip.org/content/aip/journal/jap/104/4?ver=pdfcov>

Published by the [AIP Publishing](#)

Articles you may be interested in

[Reduced leakage current and improved ferroelectricity in magneto-electric composite ceramics prepared with microwave assisted radiant hybrid sintering](#)

AIP Advances **5**, 047135 (2015); 10.1063/1.4919097

[Giant self-biased magnetoelectric response with obvious hysteresis in layered homogeneous composites of negative magnetostrictive material Samfenol and piezoelectric ceramics](#)

Appl. Phys. Lett. **103**, 202902 (2013); 10.1063/1.4829634

[Effect of B₂O₃ – Bi₂O₃ – SiO₂ – ZnO glass on the dielectric and magnetic properties of ferroelectric/ferromagnetic composite for low temperature cofired ceramic technology](#)

J. Appl. Phys. **107**, 09D911 (2010); 10.1063/1.3360347

[Magnetic field anomaly detector using magnetoelectric composites](#)

J. Appl. Phys. **101**, 024108 (2007); 10.1063/1.2427095

[Effect of composition on coupled electric, magnetic, and dielectric properties of two phase particulate magnetoelectric composite](#)

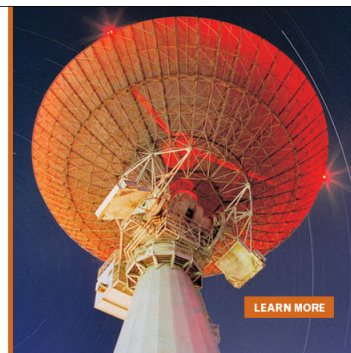
J. Appl. Phys. **101**, 014109 (2007); 10.1063/1.2404773

MIT LINCOLN
LABORATORY
CAREERS

Discover the satisfaction of
innovation and service
to the nation

- Space Control
- Air & Missile Defense
- Communications Systems & Cyber Security
- Intelligence, Surveillance and Reconnaissance Systems
- Advanced Electronics
- Tactical Systems
- Homeland Protection
- Air Traffic Control

 **LINCOLN LABORATORY**
MASSACHUSETTS INSTITUTE OF TECHNOLOGY



Giant magnetoelectric effect in sintered multilayered composite structures

Rashed A. Islam,¹ Yong Ni,² Armen G. Khachaturyan,² and Shashank Priya^{3,a)}

¹Department of Materials Science and Engineering, UT Arlington, Arlington, Texas 76019, USA

²Department of Materials Science and Engineering, Rutgers University, Piscataway, New Jersey 08854, USA

³Department of Materials Science and Engineering, Virginia Tech, Blacksburg, Virginia 24061, USA

(Received 7 May 2008; accepted 11 June 2008; published online 19 August 2008)

Trilayer composites consisting of $0.9\text{Pb}(\text{Zr}_{0.52}\text{Ti}_{0.48})\text{O}_3-0.1\text{Pb}(\text{Zn}_{1/3}\text{Nb}_{2/3})\text{O}_3$ (0.9 PZT-0.1 PZN) and $\text{Ni}_{0.6}\text{Cu}_{0.2}\text{Zn}_{0.2}\text{Fe}_2\text{O}_4$ (NCZF) in the configuration NCZF-(0.9 PZT-0.1 PZN)-NCZF were synthesized using pressure assisted sintering. Composites with optimized magnetostrictive to piezoelectric thickness ratio showed a high magnetoelectric (ME) coefficient of 525 mV/cm Oe. Further enhancement in the magnitude of ME coefficient was obtained (595 mV/cm Oe) when the angle of applied dc magnetic field was changed to 45°. Changing the intermediate piezoelectric layer from single to trilayer stack geometry configuration leads to the realization of giant ME response of 782 mV/cm Oe in sintered composites. © 2008 American Institute of Physics. [DOI: 10.1063/1.2966597]

I. INTRODUCTION

Magnetoelectric (ME) particulate composites combine the magnetostrictive and piezoelectric properties of materials^{1–3} through the product property of the system.⁴ Compared to *in situ* composite synthesized by unidirectional solidification of $\text{BaTiO}_3-\text{CoFe}_2\text{O}_4$,^{5–8} sintered particulate composite is advantageous because of its cost effectiveness, easy fabrication process, and better control of the process parameters. On the other hand laminated ME composites synthesized by using piezoelectric and magnetostrictive materials have gained attention because they exhibit superior ME response. The laminates are generally fabricated by sandwiching and bonding piezoelectric plate/disk/fibers between two layers of magnetostrictive plates/disks/foils.^{9–15} Sintered particulate composites show inferior properties compared to laminated composites because of the drawbacks such as low resistivity, interface defects, interface diffusion, mismatch in elastic compliance, and degradation in individual material parameters. Previously, we have shown that soft piezoelectric phase (high dielectric and piezoelectric constant), soft magnetic phase (high permeability and low coercivity), large piezoelectric grain size ($>1\ \mu\text{m}$), layered structure, and postsintering thermal treatment (annealing and aging) lead to the enhancement in magnitude of ME coefficient.^{16–21} In this study, we combine the advantages of layered composite with that of sintering process and investigate the geometrical and microstructural parameters that can further enhance the performance of sintered ME composites.

II. EXPERIMENTAL

Previously, we have shown that pressure assisted sintering can provide trilayer composites with any desired dimensions. Further, we have reported the compositions such that sintering can be performed at low temperature of 900 °C, which results in stable electrodes. In this study, we investi-

gate the effect of piezoelectric layer thickness in trilayer sintered ME composite upon the ME coupling. Powders of $0.9\text{Pb}(\text{Zr}_{0.52}\text{Ti}_{0.48})\text{O}_3-0.1\text{Pb}(\text{Zn}_{1/3}\text{Nb}_{2/3})\text{O}_3$ (PZT-PZN) and $\text{Ni}_{0.6}\text{Cu}_{0.2}\text{Zn}_{0.2}\text{Fe}_2\text{O}_4$ (NCZF) were synthesized using conventional mixed oxide method and trilayers were synthesized using the process described elsewhere.²²

In order to experimentally investigate the effect of thickness ratio and achieve a higher ME coefficient, composites of different piezoelectric thicknesses were synthesized. NCZF composition was used as the magnetostrictive layer and PZT-PZN composition was used as the piezoelectric layer. The amount of NCZF was fixed at 0.7 g for top and bottom layers, whereas the weight of PZT-PZN was varied from 0.8 to 0.3 g. The interface electrode used in this study was Dupont 6160 Ag-Pd conductor paste. The sintering was done at 900 °C for 3 h using a load of 450 g, which is equivalent to 50 kPa. After sintering each composite was cross sectioned and polished for scanning electron microscopy. Figure 1(a) shows the cross sections of trilayer composite. The thickness of interface electrode observed in these composites was in the range of 5–10 μm . The adherence of interface electrode with PZT-PZN and NCZF was found to be good. The PZT-PZN grain size observed in all the composites was above 1 μm . X-ray elemental analysis was performed using the scanning electron microscope in order to identify any elemental diffusion through the electroded interface. Figures 1(b)–1(d) show the elemental analysis of Pb, Fe, and Ag. A strong concentration of Pb was found on the PZT-PZN side and Fe on the NCZF side. Ag was found to be concentrated in the center region. By adding this interface electrode the piezoelectric property was improved from 80 pC/N for cofired bilayer to 225 pC/N for trilayer composite.

ME coefficient (dE/dH) was determined by applying an ac magnetic field at 1 kHz and 1 Oe amplitude (H) under varying dc magnetic bias. The ac magnetic field was generated by a Helmholtz coil powered by Agilent 3320 function generator. The output voltage generated from the composite was measured using a SRS DSP lock-in amplifier (model SR

^{a)}Electronic mail: spriya@vt.edu.

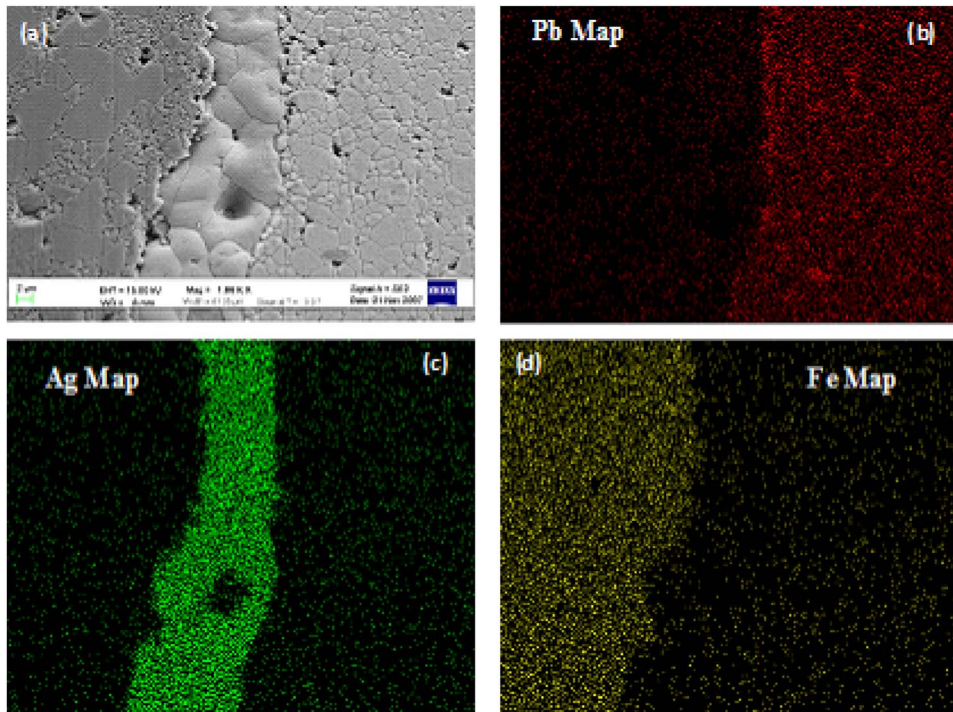


FIG. 1. (Color online) X-ray elemental mapping of trilayer sample, (a) image of trilayer sample, (b) Pb map, (c) Ag map, and (d) Fe map.

830). The ME coefficient (mV/cm Oe) was calculated by dividing the measured output voltage by thickness of the sample and applied ac magnetic field.

III. RESULTS AND DISCUSSION

The thickness ratio plays an important role in trilayer ME composites. Using the expression derived by Srinivasan *et al.*²³ it can be shown that the ME coefficient depends on piezoelectric coefficient (d_{31}), permittivity (ϵ_{33}), elastic com-

pliance (s_{11} and s_{12}), thickness (t_p) of the piezoelectric phase, piezomagnetic coefficient (q_{11}), elastic compliance (s_{11} and s_{12}), and thickness (t_m) of the magnetic phase as the following:

$$\frac{\delta E_3}{\delta H_1} = \frac{-2d_{31}^p q_{11}^m \frac{t_m}{t_p}}{(s_{11}^m + s_{12}^m)\epsilon_{33}^{T,P} + (s_{11}^p + s_{12}^p)\epsilon_{33}^{T,P} \frac{t_m}{t_p} - 2(d_{31}^p)^2 \frac{t_m}{t_p}}. \quad (1)$$

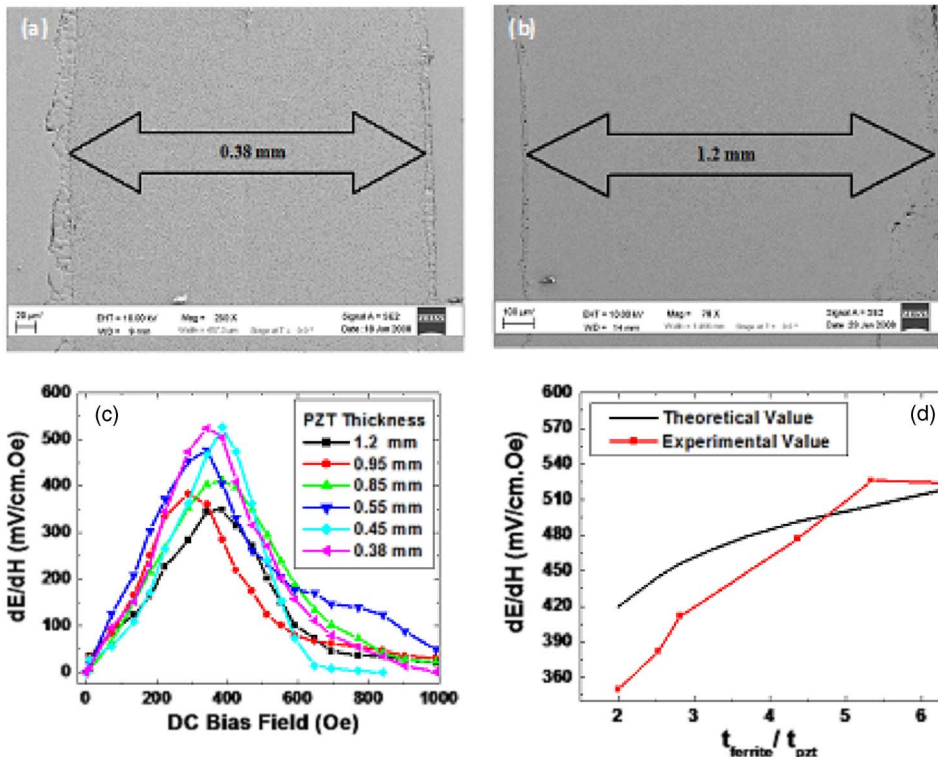


FIG. 2. (Color online) (a) Trilayer composite with piezoelectric layer thickness of 0.38 mm, (b) trilayer composite with piezoelectric layer thickness of 1.2 mm, (c) ME coefficient as a function of dc bias field for different thicknesses of piezoelectric layer, and (d) comparison between theoretical and experimental ME coefficients for different thickness ratios of magnetic to piezoelectric layer.

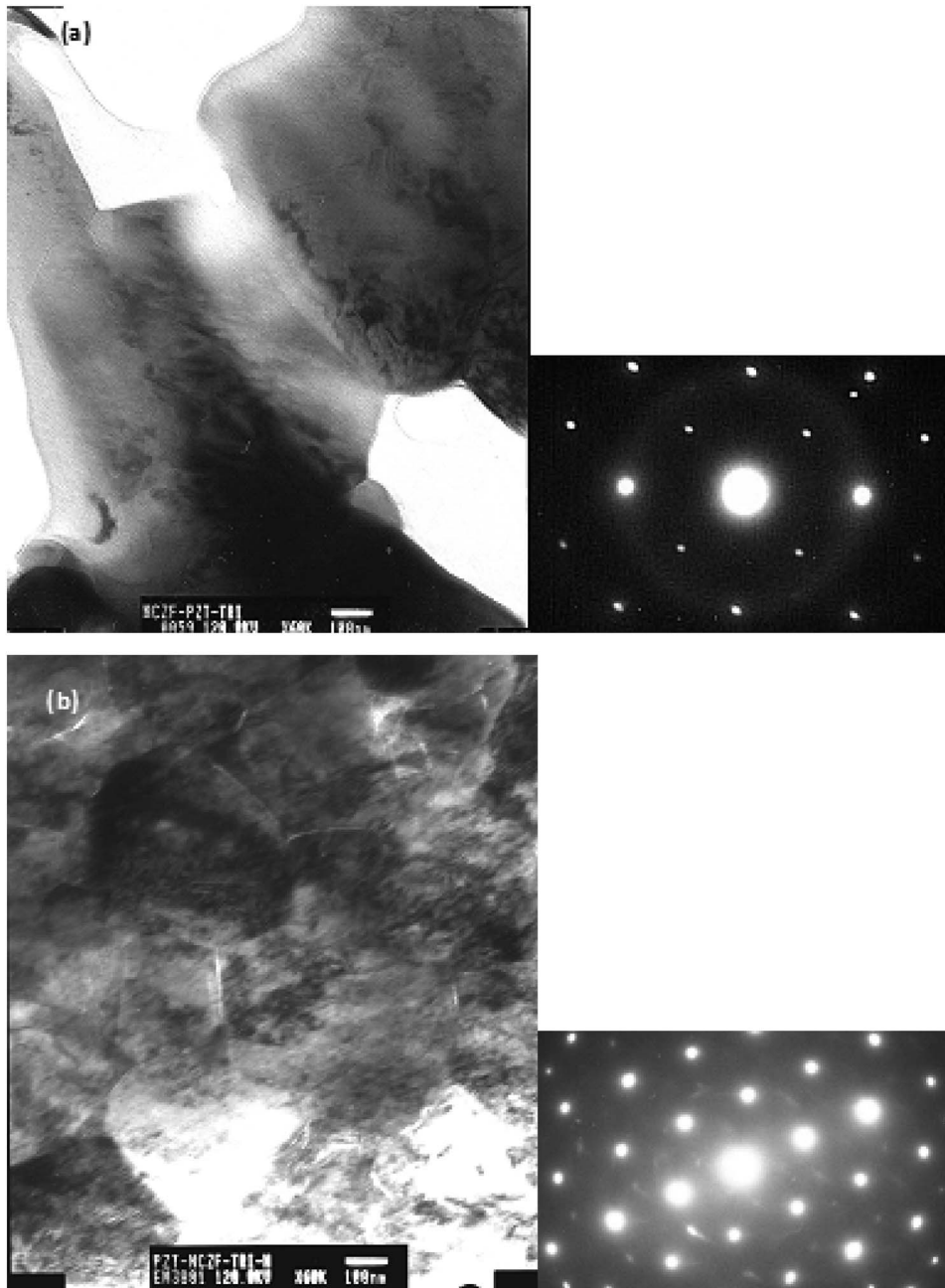


FIG. 3. TEM micrograph and SAED pattern for (a) PZT-PZN and (b) NCZF near the interface in trilayer composites.

Equation (1) shows that ME coefficient is a function of magnetostrictive to piezoelectric layer thickness ratio. Figures 2(a) and 2(b) show the cross-section image of trilayer composite with different thicknesses of the piezoelectric phase. Figure 2(c) shows the ME coefficient as a function of dc bias field for different thicknesses of piezoelectric layer. It was found that as the thickness ratio of magnetic layer to piezoelectric layer increases (thickness of piezoelectric layer decreases as the magnetic layer thickness was fixed) ME coefficient increases from 354 to 526 mV/cm Oe. The maximum ME coefficient of 526 mV/cm Oe was found when the thickness ratio was 5.3 (piezoelectric layer thickness was 0.45 mm).

The calculated theoretical magnitude of ME coefficient using Eq. (1) is plotted along with the experimental values in Fig. 2(d). The experimental values were found to have close resemblance with the prediction from theory. The ME coef-

ficient was of the order of 350 mV/cm Oe for piezoelectric layer thickness of 1.2 mm (ratio of 2) and it increases as the ratio increases. The increase in ME coefficient and the decrease in piezoelectric layer thickness can be explained in terms of increased compressive stress on piezoelectric layer.

Ryu *et al.*³ have shown that the compressive and tensile stresses in piezoelectric and ferrite layers can be calculated using the beam theory given as

$$\sigma_{31f}^E = \frac{E_f E_p t_p \Delta \epsilon_o}{(1 - \gamma)(2E_f t_f + E_p t_p)}, \quad (2)$$

$$\sigma_{31p}^E = - \frac{2E_f E_p t_p \Delta \epsilon_o}{(1 - \gamma)(2E_f t_f + E_p t_p)}. \quad (3)$$

As the thickness of ferrite layer remains the same (1.2 mm on top and bottom), the compressive stress on piezoelectric

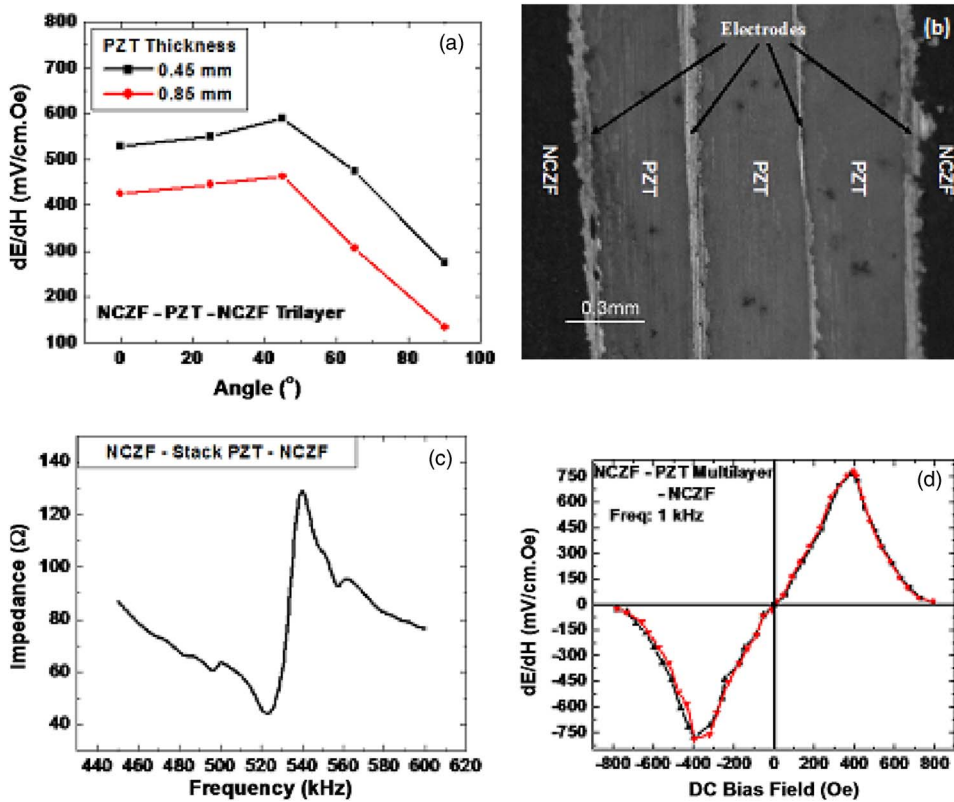


FIG. 4. (Color online) (a) Effect of orientation on ME coefficient of NCZF-(PZT-PZN)-NCZF trilayer composite with two different piezoelectric layer thicknesses, (b) cross-sectional optical image of NCZF-stack (PZT-PZN)-NCZF trilayer, (c) impedance spectrum for NCZF-stack (PZT-PZN)-NCZF trilayer, and (d) ME coefficient of NCZF-stack (PZT-PZN)-NCZF trilayer.

layer can be increased if the thickness of piezoelectric layer is decreased. The compressive stress is related to ME coefficient as³

$$\frac{dE}{dH} = \frac{2g_{31}\sigma_{31P}^E}{H_{ac}} \quad (4)$$

Thus, as the compressive stress in piezoelectric is increased, ME coefficient increases.

Figures 3(a) and 3(b) show the transmission electron microscopy (TEM) micrographs of PZT-PZN and NCZF phases close to the interface. The inset of each image shows the selected area electron diffraction (SAED) pattern. The micrographs were taken within 10 μm from the interface on both sides. From the diffraction pattern, pure piezoelectric and magnetic phases can be identified. The grain sizes observed in these micrographs were around 1 μm for piezoelectric phase and ~ 500 nm for NCZF phases. The lattice parameters calculated from SAED pattern were found to be $a = 4.04$ \AA and $c = 4.11$ \AA with tetragonality (c/a ratio) of 1.017. The lattice constant for NCZF was calculated to be 8.41 \AA . This clearly signifies that the interface diffusion was limited in the trilayer. The interface diffusion length observed in the case of bilayer composite was around 30 μm , which did not consist of intermediate electrode. Thus, trilayer geometry with intermediate electrode layer was able to reduce the interface diffusion.

Figure 4(a) shows the magnetic field (ac and dc) orientation dependence of ME coefficient for trilayer composite (piezoelectric layer thicknesses of 0.45 and 0.85 mm). It was found that the composite shows an increase in ME coefficient from 0° (when magnetic field direction is parallel to the sample surface) to 45°. The maximum ME coefficients of

589 and 463 mV/cm Oe were measured at 45° orientation. As the angle is increased beyond 45°, the ME coefficient starts to drop rapidly and when the sample surface is perpendicular to the magnetic field direction (T-T mode), low values of 274 and 134 mV/cm Oe were observed for two different thicknesses of piezoelectric layer. It has been shown that with areal angle change, the strain of the magnetic phase changes and is maximum around 51°. ²⁴ As the strain increases compressive stress on piezoelectric layer also increases, which contributes to the high ME coefficient as expressed by Eq. (4). At 90° angle the ME coefficient was found to have low magnitude.

In trilayer ME composite based on NCZF-(PZT-PZN)-NCZF composition, the optimum magnitude of d_{33} and dielectric constant were found to be 225 pC/N and 1150. In order to achieve higher piezoelectric and dielectric constants, it is necessary to change the electrode pattern of the piezoelectric layer. Thus, a stack actuator configuration was implemented in trilayer geometry as intermediate layer between two NCZF layers. Figure 4(b) shows the optical image of new trilayer design with stacked PZT-PZN configuration. It can be seen from this figure that instead of single PZT-PZN layer there were three PZT-PZN layers and corresponding interdigital electrode layers along thickness direction. The sintering temperature and time were 900 °C for 3 h with very slow heating and cooling rates (~ 1 °C/min). Pressure applied during the sintering was 50 kPa to avoid any delamination. It was found that each layer of PZT-PZN was around 300 μm combined with a thickness of 0.9 mm. NCZF layers were found to have a thickness of 1.2 mm.

In the above configuration, piezoelectric constant (d_{33}) increased from 204 to 535 pC/N and dielectric constant from

1132 to 5500. However, the dielectric loss of stack PZT-PZN increased from 5% to 13.4%, which may be due to incomplete sintering of Ag-Pd electrode and PZT-PZN. The increase in electromechanical coupling constant from 0.14 to 0.21 was observed, which indicates that there was minimal mechanical defect in the fabricated structure. Figure 4(c) shows the impedance spectrum of trilayer ME composite. The resonance frequency was measured to be 523 kHz, which is higher than that of single layer PZT-PZN and shows resonance at 258 kHz for the same dimensions. Also the bandwidth (difference between resonance and antiresonance) was found to be higher (17 kHz) in the case of trilayer composite with stack actuator configuration.

Figure 4(d) shows the ME coefficient of stack PZT-PZN based trilayer composite. It shows a peak coefficient of 782 mV/cm Oe at 400 Oe magnetic dc bias. In order to check whether there is any hysteresis behavior, the ME coefficient was measured from negative to positive high field and vice versa. It was found that there is very small hysteresis in the response. Compared to the single layer PZT-PZN in trilayer configuration (412 mV/cm Oe), stack PZT-PZN shows much higher ME coefficient. This is a significant improvement in the performance of the sintered ME composites.

IV. SUMMARY

NCZF-(0.9 PZT-0.1 PZN)-NCZF trilayer was fabricated using pressure assisted sintering. Optimization of ferrite to PZT-PZN layer thickness was done in order to find the most favorable thickness ratio. It was found that for PZT-PZN layer thickness of 0.45 mm (ferrite to PZT-PZN thickness ratio of 5.33) the ME coefficient increases from 412 (for PZT-PZN thickness 0.85) to 526 mV/cm Oe. Optimization of magnetic field orientation measurement shows that if the angle between the magnetic field direction and the sample surface is 45°, the ME coefficient magnitude reaches 589 mV/cm Oe (for 0.45 mm PZT thickness). Instead of a

single PZT-PZN layer if a stack configuration was adopted, a significant improvement in ME coefficient was obtained.

ACKNOWLEDGMENTS

The authors gratefully acknowledge the financial support from Office of Basic Energy Sciences, Department of Energy. The authors (R.I. and S.P.) would also like to acknowledge the support from Army Research Office.

- ¹J. Van Suchtelene, Philips Res. Rep. **27**, 28 (1972).
- ²J. Ryu, S. Priya, K. Uchino, D. Viehland, and H. Kim, J. Kor. Ceram. Soc. **39**, 813 (2002).
- ³J. Ryu, S. Priya, and K. Uchino, *J. Electroceram.* **8**, 107 (2002).
- ⁴G. R. Harshe, Ph.D. thesis, Pennsylvania State University, 1991.
- ⁵J. V. D. Boomgaard and R. A. J. Born, *J. Mater. Sci.* **13**, 1538 (1978).
- ⁶J. V. D. Boomgaard, D. R. Terrell, R. A. J. Born, and H. F. J. I. Giller, *J. Mater. Sci.* **9**, 1705 (1974).
- ⁷A. M. J. G. Van Run, D. R. Terrell, and J. H. Scholing, *J. Mater. Sci.* **9**, 1710 (1974).
- ⁸J. V. D. Boomgaard, A. M. J. G. Van Run, and J. Van Suchtelen, *Ferroelectrics* **10**, 295 (1976).
- ⁹S. Dong, J. Li, and D. Viehland, *Appl. Phys. Lett.* **83**, 2265 (2003).
- ¹⁰S. Dong, J. Zhai, J. Li, and D. Viehland, *Appl. Phys. Lett.* **89**, 252904 (2006).
- ¹¹G. Srinivasan and Y. K. Fetisov, *Ferroelectrics* **342**, 65 (2006).
- ¹²R. Zhang, M. Wang, N. Zhang, and G. Srinivasan, *Acta Phys. Sin.* **55**, 2548 (2006).
- ¹³Z. Shi, J. Ma, Y. H. Lin, and C. W. Nan, *J. Appl. Phys.* **101**, 043902 (2007).
- ¹⁴S. Dong, J. Zhai, J. F. Li, D. Viehland, and M. I. Bichurin, *Appl. Phys. Lett.* **89**, 243512 (2006).
- ¹⁵D. A. Filippov, M. I. Bichurin, C. W. Nan, and J. M. Liu, *J. Appl. Phys.* **97**, 113910 (2005).
- ¹⁶R. A. Islam and S. Priya, *Integr. Ferroelectr.* **82**, 1 (2006).
- ¹⁷R. A. Islam and S. Priya, *Jpn. J. Appl. Phys., Part 2* **45**, L128 (2006).
- ¹⁸R. A. Islam and S. Priya, *Int. J. Appl. Ceram. Technol.* **3**, 353 (2006).
- ¹⁹R. A. Islam, D. Viehland, and S. Priya, *J. Mater. Sci. Lett.* **43**, 1497 (2008).
- ²⁰R. A. Islam, and S. Priya, *J. Mater. Sci.* **43**, 3560 (2008).
- ²¹R. A. Islam, J. C. Jiang, S. Priya, F. Bai, and D. Viehland, *Appl. Phys. Lett.* **91**, 162905 (2007).
- ²²R. A. Islam and S. Priya, *J. Mater. Sci.* **43**, 2072 (2008).
- ²³G. Srinivasan, E. Rasmussen, J. Gallegos, R. Srinivasan, Y. I. Bokhan, and V. M. Laletin, *Phys. Rev. B* **64**, 214408 (2001).
- ²⁴J. Ryu, S. Priya, A. V. Carazo, K. Uchino, and H. Kim, *J. Am. Ceram. Soc.* **84**, 2905 (2001).